AEM
Journals.ASM.org

Mercury Resistance and Mercuric Reductase Activities and Expression among Chemotrophic Thermophilic *Aquificae*

Zachary Freedman,[a,b]* Chengsheng Zhu,[a] and Tamar Barkay[a,b]

Department of Biochemistry and Microbiology[a] and Graduate Program in Ecology and Evolution,[b] Rutgers University, New Brunswick, New Jersey, USA

Mercury (Hg) resistance (*mer*) by the reduction of mercuric to elemental Hg is broadly distributed among the *Bacteria* and *Archaea* and plays an important role in Hg detoxification and biogeochemical cycling. MerA is the protein subunit of the homodimeric mercuric reductase (MR) enzyme, the central function of the *mer* system. MerA sequences in the phylum *Aquificae* form the deepest-branching lineage in Bayesian phylogenetic reconstructions of all known MerA homologs. We therefore hypothesized that the *merA* homologs in two thermophilic *Aquificae*, *Hydrogenobaculum* sp. strain Y04AAS1 (AAS1) and *Hydrogenivirga* sp. strain 128-5-R1-1 (R1-1), specified Hg resistance. Results supported this hypothesis, because strains AAS1 and R1-1 (i) were resistant to >10 μM Hg(II), (ii) transformed Hg(II) to Hg(0) during cellular growth, and (iii) possessed Hg-dependent NAD(P)H oxidation activities in crude cell extracts that were optimal at temperatures corresponding with the strains' optimal growth temperatures, 55°C for AAS1 and 70°C for R1-1. While these characteristics all conformed with the *mer* system paradigm, expression of the *Aquificae mer* operons was not induced by exposure to Hg(II) as indicated by unity ratios of *merA* transcripts, normalized to *gyrA* transcripts for hydrogen-grown AAS1 cultures, and by similar MR specific activities in thiosulfate-grown cultures with and without Hg(II). The Hg(II)-independent expression of *mer* in the deepest-branching lineage of MerA from bacteria whose natural habitats are Hg-rich geothermal environments suggests that regulated expression of *mer* was a later innovation likely in environments where microorganisms were intermittently exposed to toxic concentrations of Hg.

Microbes must have been exposed to toxic heavy metals since the beginning of life on Earth and have evolved diverse mechanisms to live in the presence of high concentrations of toxic metal ions (42). These mechanisms, such as efflux, intra- or extracellular precipitation, and enzyme-mediated transformations, control intracellular concentrations of heavy metal ions that may be inhibitory to physiological functions and form nonspecific complex compounds in the cell (28). While much of our existing knowledge of these resistance mechanisms has arisen from research motivated by metal contamination from the perspective of human and environmental health (5, 9, 11, 26, 29), a cosmopolitan distribution of metal-resistant microorganisms inhabiting environments that are enriched with metals of geological origin suggests evolution of metal ion resistance prior to industrial release of metal contaminants (2, 13, 50).

Mercury (Hg) is a potent neurotoxic substance and the heavy metal most toxic to microorganisms due to its high affinity to sulfur (27). Globally distributed Hg (3) is toxic to humans and wildlife, mostly due to the accumulation of methylmercury (MeHg) in aquatic and terrestrial food webs (7). Microbial activities are central in modulating environmental Hg toxicity and mobility. Resistance to inorganic Hg [Hg(II)] is controlled by the activities of the enzyme mercuric reductase (MR), an NAD(P)H-dependent flavin oxidoreductase which catalyzes the reduction of Hg(II) to the elemental form, Hg(0). The gene encoding MR, *merA*, is part of the Hg resistance (*mer*) operon, which is widespread among both *Bacteria* and *Archaea* (2, 3, 43), allowing these organisms to survive in the presence of elevated Hg concentrations (3, 4). At a minimum, Hg resistance systems are comprised of transport, enzymatic, and regulatory functions. MerT and a number of alternative transporters are involved in the transport of thiolated Hg(II) into the cytoplasm for reduction by MR (3). MerR regulates expression of the *mer* operon, binding to the operator/promoter (O/P) region to repress transcription in the absence of Hg(II). When present, Hg(II) binds to the MerR-*mer* O/P and RNA polymerase complex, prompting the DNA to unwind, inducing transcription of the operon's functional genes (3, 17).

A recent body of literature supports the hypothesis that microbial resistance to Hg evolved in geothermal environments where microbial life has perhaps been exposed to Hg since the beginning of life on Earth (2, 35, 48). Mercury-resistant microbes were readily isolated from deep-sea hydrothermal vents (48) and terrestrial hot springs (10, 43), and their distribution suggested a role in adaptation to Hg toxicity. Culture-independent techniques detected *mer* genes in Yellowstone National Park (YNP) (50) and Coso Hot Springs, CA (43). The large-scale sequencing of microbial genomes has resulted in an increased availability of *merA* sequences and allowed for a robust analysis of gene evolution, further supporting an origin and early evolution of Hg resistance among thermophilic microbes from geothermal environments (2).

To date, functional *mer* operons have been characterized in mesophilic *Actinobacteria*, in *Firmicutes*, among the *Beta-* and *Gammaproteobacteria* (2), and in one thermophilic bacterium representing an early bacterial lineage, *Thermus thermophilus* HB27 (51). The phylum *Aquificae* contains primary producers which are dominant in many geothermal environments (46) and

Received 31 March 2012 Accepted 1 July 2012
Published ahead of print 6 July 2012
Address correspondence to Tamar Barkay, barkay@aesop.rutgers.edu.
* Present address: Zachary Freedman, School of Natural Resources and Environment, University of Michigan, Ann Arbor, Michigan, USA.
Supplemental material for this article may be found at http://aem.asm.org/.

doi:10.1128/AEM.01060-12

represents the deepest-branching bacterial lineage (23). Furthermore, *merA* homologs in the genomes of *Hydrogenobaculum* sp. strain Y04AAS1 (AAS1) and *Hydrogenivirga* sp. strain 128-5-R1-1 (R1-1) (34) form the deepest-branching lineage in a MerA phylogeny (2). Strain AAS1 was isolated from a small channel proximal to Obsidian Pool Prime, YNP, and R1-1 was isolated from the Eastern Lau Spreading Center, South Pacific (34), both of which are geothermal environments similar to those where elevated Hg concentrations were reported (12, 21, 31). The basal position of the *Aquificae* loci in the MerA phylogenetic reconstructions suggests that *merA* originated in an ancestor common to deep-branching thermophilic bacteria. Here, we report on the activity and characteristics of the Hg resistance systems of two *Aquificae* strains representing chemotrophic primary producers in many geothermal environments.

MATERIALS AND METHODS

MerA phylogeny and bioinformatic analyses. MerA sequences were compiled in April 2011 by tblastx searches of the Entrez Protein database (http://www.ncbi.nlm.nih.gov/sites/entrez?db=protein) using the MerA amino acid sequences of Tn*501* (accession number CAA77323.1) and *Sulfolobus solfataricus* P2 (AAK42805.1) as queries. These searches identified two open reading frames (ORFs), HY04AAS1_1213 and HG1285_05690, as *merA* homologs in *Hydrogenobaculum* sp. Y04AAS1 and *Hydrogenivirga* sp. 128-R1-1, respectively. The alignment block of bacterial and archaeal MerA sequences, corresponding to positions 8 to 472 of *Streptomyces lividans* (P30341), were used in a Bayesian inferred phylogenetic reconstruction, performed as described by Wang et al. (50). Of the 284 gene homologs available, 99 were selected for reconstruction; the selected homologs represented all major clusters in the MerA phylogeny. Putative promoter regions were determined using the BPROM tool (Softberry Inc., Mt. Kisco, NY).

Bacterial strains and growth conditions. Strains *Hydrogenobaculum* sp. Y04AAS1 (AAS1), *Hydrogenivirga* sp. 128-5-R1-1 (R1-1), and *Persephonella marina* EX-H1 were generously provided by Anna-Louise Reysenbach (Portland State University); major characteristics of these strains are summarized in Table S1 in the supplemental material. All growth media were prepared under a CO_2 headspace, microaerophilic conditions were then created by the postautoclaving addition of O_2 (to 4%, vol/vol), and the tubes were pressurized with either H_2 or CO_2 after inoculation. Strain AAS1 was grown at 55°C in modified DSMZ 743 medium (Boone's medium no. 5) as described by Shima and Suzuki (41), supplemented with 0.5 ml liter^{-1} of a trace element stock solution (adapted from Ferguson and Mah [15]). Elemental sulfur was replaced in this medium with $S_2O_3^{2-}$ or H_2 as the energy source, and the pH was adjusted to 4.5 with 6 N HCl prior to autoclaving. Strains R1-1 and EX-H1 were grown at 70°C in modified MSH medium (Boone's medium no. 2) (6) supplemented with 10 ml liter^{-1} of trace element stock solution, with pH adjusted to 6.0 with 6 M H_2SO_4. The headspace consisted of 96:4 CO_2/O_2 and 80:16:4 $CO_2/H_2/O_2$ when grown on $S_2O_3^{2-}$ and H_2 as electron donors, respectively. In both media, $S_2O_3^{2-}$ was omitted when H_2 was provided as the sole electron donor, whereas no H_2 was added to the headspace when $S_2O_3^{2-}$ was used. Strain R1-1, which grew poorly with H_2, was tested only in $S_2O_3^{2-}$-amended medium. Unless specifically described, all culture maintenance and growth experiments were performed in a final volume of 5 ml in 26-ml Balch tubes (Bellco, Vineland, NJ) fitted with crimp-sealed Teflon stoppers.

Growth measurements. Growth was determined by measuring the optical density at a wavelength of 660 nm (A_{660}) (Genesys 20; Thermo Spectronic Instruments, Waltham, MA) or by acridine orange direct counts (49). For direct count preparations of strain *Hydrogenobaculum* sp. Y04AAS1, acridine orange staining was carried out following cell filtration onto polycarbonate filters (General Electric, Feasterville-Trevose, PA) to minimize staining of medium precipitates. Cell numbers were obtained using an Olympus BX60 microscope with an oil immersion objective lens (Uplan F1 100×/1.3) and determined using Olympus Microsuite Basic (version 3.2) (Olympus Corp, Center Valley, PA).

Modeling of Hg speciation. The chemical equilibrium speciation model MINEQL+ (version 4.5) (38) was used to determine the speciation of Hg in growth media. Input parameters were obtained from the MINEQL+ and the National Institute of Standards and Technology databases (24). Dissociation constants used as input parameters are shown in Table S2 in the supplemental material. Hg speciation in each growth medium was modeled at a $HgCl_2$ concentration range of 5 to 60 μM.

Resistance to Hg(II). Mid-log-phase cultures were diluted 100-fold into fresh growth medium to a final volume of 5 ml at an A_{660} of 0.010, $HgCl_2$ was added to a final concentration of 0, 5, 10, 20 or 40 μM, and tubes were incubated at each organism's optimal growth temperature in the dark without shaking. Growth was monitored every 4 to 8 h until commencement of stationary phase. The effect of Hg on growth was expressed as cell density at a given $HgCl_2$ concentration as a percentage of cell density of the zero-$HgCl_2$ control when the control culture approached late exponential growth, with 5.3×10^7 and 2.8×10^7 cells ml^{-1} for strain AAS1 growing on $S_2O_3^{2-}$ and H_2, respectively, and 2.6×10^7 cells ml^{-1} for $S_2O_3^{2-}$-grown cultures of strain R1-1.

Loss of Hg(II) during culture growth. Fresh growth media were inoculated with mid-log-phase cultures and were spiked with 5 or 10 μM $^{203}HgCl_2$ (specific activity, 0.5 to 0.12 nCi [μmol Hg]$^{-1}$; kindly provided by Christie Bridges [Mercer University, GA]) for cultures grown on H_2 or $S_2O_3^{2-}$, respectively. ^{203}Hg remaining in growth media was monitored by removing 250-μl aliquots from growing cultures every 4 to 8 h to 3 ml of Scinti-Verse scintillation fluid (Thermo Fisher Scientific, Waltham, MA), and samples were counted in a Beckman LS 6500 liquid scintillation counter (Beckman-Coulter, Brea, CA). Growth was measured in parallel cultures containing unlabeled $HgCl_2$ at similar concentrations.

Maximum apparent specific Hg loss rates [fmol Hg(II) lost h^{-1} cell^{-1}] were calculated as $([Hg_{t1} - Hg_{t2}]/[t_2 - t_1])N^{-1}$, where N is the average number of cells at t_1 and t_2, Hg is fmol of Hg(II) lost between t_1 and t_2 as calculated from the concentration of Hg that remained in the growth medium at t_1 and t_2, and t_1 and t_2 are the times (h) bracketing the interval at which the loss of ^{203}Hg from the medium was the greatest (37). Controls included autoclaved cells (105°C, 30 min) with identical inoculum sizes to test cultures as well as uninoculated media. Significance ($P < 0.05$) of differences in Hg(II) loss rates for each treatment was calculated using Student's t test.

Production of Hg(0) by growing cultures. Cultures were grown with $^{203}HgCl_2$ as described above to stationary phase when the headspace of the incubation vessels was flushed with sterile air for 40 min to drive ^{203}Hg(0) that accumulated during growth into a Hg-trapping solution consisting of 0.75% $KMnO_4$, 0.40% $K_2S_2O_3$, 3.5% HNO_3, and 5% H_2SO_4. At the conclusion of the 40 min, the remaining growth medium was acidified to 0.5 N HCl and mixed by vortexing. Aliquots of 250 μl were removed from the acidified stationary-phase culture and the trapping solution for scintillation counting. Control treatments included autoclaved cells and uninoculated growth medium.

Mercuric reductase (MR) assays. Mid-log-phase cultures of *Hydrogenobaculum* sp. Y04AAS1 and *Hydrogenivirga* sp. 128-R1-1 were diluted 100-fold into 250 ml of medium in rubber-capped 2-liter Pyrex medium bottles (Corning, Lowell, MA) with a microaerophilic headspace as described under "Bacterial strains and growth conditions" above. Cultures were grown to mid-log phase, and cells were harvested by centrifugation for 10 min at 5,750 × g at 4°C in a prerefrigerated Sorvall RC-5B centrifuge (Thermo Scientific, Waltham, MA). Pelleted cells were washed in phosphate-buffered saline and stored at −20°C until used for further analysis.

Cell-free lysates were prepared by following protocols described by Vetriani et al. (48). Cells were resuspended to a concentration of 200 mg ml^{-1} (wet weight) in a buffer consisting of 20 mM sodium phosphate (pH 7.5), 0.5 mM EDTA, and 1 mM β-mercaptoethanol and were lysed by

intermittent sonication using a Misonex S-4000 sonicator (Misonex, Newtown, CT) for a total of 3 min on ice. MR assays were performed in 80 mM sodium phosphate buffer (pH 7.4) with 1 mM β-mercaptoethanol, 200 μM NAD(P)H, and 50 μM $HgCl_2$ in a final volume of 800 μl (16). Mercury-dependent NAD(P)H oxidation was monitored as the decrease in A_{340} using a UV-visible (UV-Vis) spectrophotometer (Cary 300; Agilent Technologies, Budd Lake, NJ). Assay temperatures were controlled using a water-jacketed cuvette holder connected to a water bath. Cell extracts and test buffer were preincubated at the assay temperature for 10 min prior to the addition of 1 to 4 μl of extract to the assay buffer. Initial rates of NAD(P)H oxidation were determined in the first 10 s, when the A_{340} decreased linearly with time. At least 3 different extract concentrations were tested, once with and once without the addition of $HgCl_2$. Specific Hg-dependent NAD(P)H oxidation rates, expressed as units mg protein^{-1} [1 U = 1 μmol of NAD(P)H oxidized min^{-1}], were calculated by subtracting the slope of the curve obtained in the absence of $HgCl_2$ from that observed following $HgCl_2$ addition. Protein concentrations in crude cell extracts were determined using the Bradford assay (Bio-Rad Laboratories Inc., Hercules, CA).

The effect of growth with and without Hg on MR levels of AAS1 and R1-1 was determined as described above except that treated cultures were grown with 10 μM $HgCl_2$ on $S_2O_3^{2-}$. An additional 10 μM $HgCl_2$ was added at mid-log phase, followed by continued incubation for 2 doubling times prior to cell harvesting. Significance ($P < 0.05$) of differences in MR activities among treatments was calculated by Student's *t* test.

Induction of *merA* transcription. Cultures of R1-1 and AAS1 were grown in 25 ml of medium in 125-ml serum bottles (Wheaton Scientific, Millville, NJ). When the culture approached mid-log phase, 1 μM $HgCl_2$ was added ($t = 0$), and 1.5-ml samples were withdrawn at 0, 10, 30, and 60 min. Cells were harvested by centrifugation (1 min, 13,000 × *g*) and immediately frozen at −80°C. Control cultures (zero Hg) were included to determine basal levels of *merA* transcription. Total RNA was extracted using the TRIzol reagent (Invitrogen, Carlsbad, CA) and diluted to 20 μg ml^{-1} prior to DNase treatment with the Turbo DNA-free kit (Applied Biosystems, Carlsbad, CA) as recommended in the manufacturer's instructions. cDNA was synthesized using the High-Capacity cDNA reverse transcription (RT) kit (Applied Biosystems) using a GeneAmp PCR System 9700 (Applied Biosystems) thermocycler. Relative *merA* fold induction was measured by quantitative real-time PCR (qPCR) using cDNA as a template and was normalized to transcription levels of *gyrA*, a constitutively expressed gene. No RT controls were performed to rule out the presence of DNA contamination.

For *Hydrogenobaculum* sp. Y04AAS1, primers RT-HBmerA(f/r) and HBgyrA(f/r) were used to amplify 71- and 66-bp regions of *merA*- and *gyrA*-specific products, respectively (see Table S3 in the supplemental material). For *Hydrogenivirga* sp. 128-R1-1, RT-HVmerA(f/r) and HVgyrA(f/r) were used to produce 70-bp *merA*-specific and 107-bp *gyrA*-specific products, respectively. Primers were designed using default parameters within Primer Express (version 3.0) (Applied Biosystems), using *merA* and *gyrA* sequences in the genomes of AAS1 (*gyrA* locus HY04AAS1_0371) and R1-1 (*gyrA* locus HG1285_00715). The Power SYBR green PCR master mix (Applied Biosystems) was used in all qPCRs. Amplifications were performed in triplicate for both *merA* and *gyrA* transcripts using the StepOne Plus PCR machine running StepOne software (version 2.1) (Applied Biosystems). qPCR conditions included an initial denaturation step of 90°C for 10 min and then 45 cycles of 90°C for 15 s followed by 1 min at 55°C for all primer sets used. Upon completion, a melt curve was performed to verify identity of the amplification products. Relative induction levels were calculated by the comparative threshold cycle (C_T) method (30), whereby expression of *merA* was related to that of *gyrA* in cultures grown with and without Hg. ΔC_T values were obtained for each time point following the addition of $HgCl_2$ to exposed cultures.

RESULTS AND DISCUSSION

Identification of putative *mer* operons in the genomes of *Hydrogenobaculum* sp. Y04AAS1 and *Hydrogenivirga* sp. 128-5-R1-1. An updated phylogeny that included all MerA homologs in databases as of April 2011 confirmed (2) the basal position of the *Aquificae* sequences in a sister position to all archaeal sequences with posterior probability values of 100. This cluster shared a common, likely bacterial, ancestor with a large cluster consisting of the remaining bacterial MerA sequences (see Fig. S1 in the supplemental material). These results highlight the important position of the *Aquificae* MerA, potentially representing an ancestral state of the protein among all prokaryotes.

The MerA sequences of both *Aquificae* loci contained signature motifs known to be required for MerA activity (Fig. 1A) (3). In *Hydrogenobaculum* sp. Y04AAS1, MerA is 464 amino acids (aa) long, while in *Hydrogenivirga* sp. 128-R1-1, it is 545 residues long due to the presence of NmerA, the ~70-aa N-terminal extension heavy metal-associated (HMA) domain that is a part of more than half of all MerA sequences (2). Mercuric reductase activities were documented for both variants of MerA (51), and NmerA is not essential for MerA activity (22).

In both *Aquificae* strains, two ORFs upstream of the putative *merA* code for proteins that bear homology to other Mer functions (Fig. 1B). The *merA*-proximal ORFs, loci YP_002121875 (78 aa) and ZP_02177251 (92 aa) in the genomes of strains AAS1 and R1-1, respectively, may encode the Hg-scavenging protein MerP, as they include the signature metal binding motif sequence GMTCxxC (Fig. 1A). However, the ~19-residue *Sec*-type signal known to direct proteobacterial MerP to the periplasmic space (3, 20) is missing in both *Aquificae* loci, leaving in question the transport of their gene products to the periplasmic space and thus their function as MerP.

ORFs encoding MerT homologs are found upstream of the putative *merP* genes in both genomes (loci HY04AAS1_1211 and ZP_02177250 [Fig. 1A]). Homology includes three hydrophobic inner membrane-spanning sequences as determined by TMpred (18), the vicinal C pair in the first membrane-spanning sequence, and a C pair located in the cytoplasmic loop between the second and the third membrane-embedded sequences (36).

Homologs of the *mer* operon regulator, MerR, were not found in the genomes of strains AAS1 and R1-1, though several homologs of ArsR/SmtB, a regulator reported in *mer* systems of the *Archaea* and the *Actinobacteria* (2, 3), were identified using tBLASTn searches. Based on homology searches, putative promoter regions (33) were identified 26 and 15 bp upstream of the ATG start codon of the ORFs preceding *merT* in strains *Hydrogenobaculum* sp. Y04AAS1 and *Hydrogenivirga* sp. 128-R1-1, respectively. These included −35 and −10 regions (separated by 16 and 17 nucleotides, rather than by 19 nucleotides as is common to promoters that are regulated by MerR [8]), Shine-Dalgarno ribosomal binding sites, and translation initiation signals. No other possible promoter sequences were identified upstream of any of the *mer* homologs of these strains.

Mercury resistance in *Hydrogenobaculum* sp. AAS1, *Hydrogenivirga* R1-1, and *Persephonella marina* EX-H1. The technology to genetically manipulate bacteria that belong to the *Aquificae* is not yet available, and thus, obtaining *merA* mutants of strains AAS1 and R1-1 was not possible. We therefore compared Hg tolerance in strains AAS1 and R1-1 to that of *P. marina* EX-H1 as a

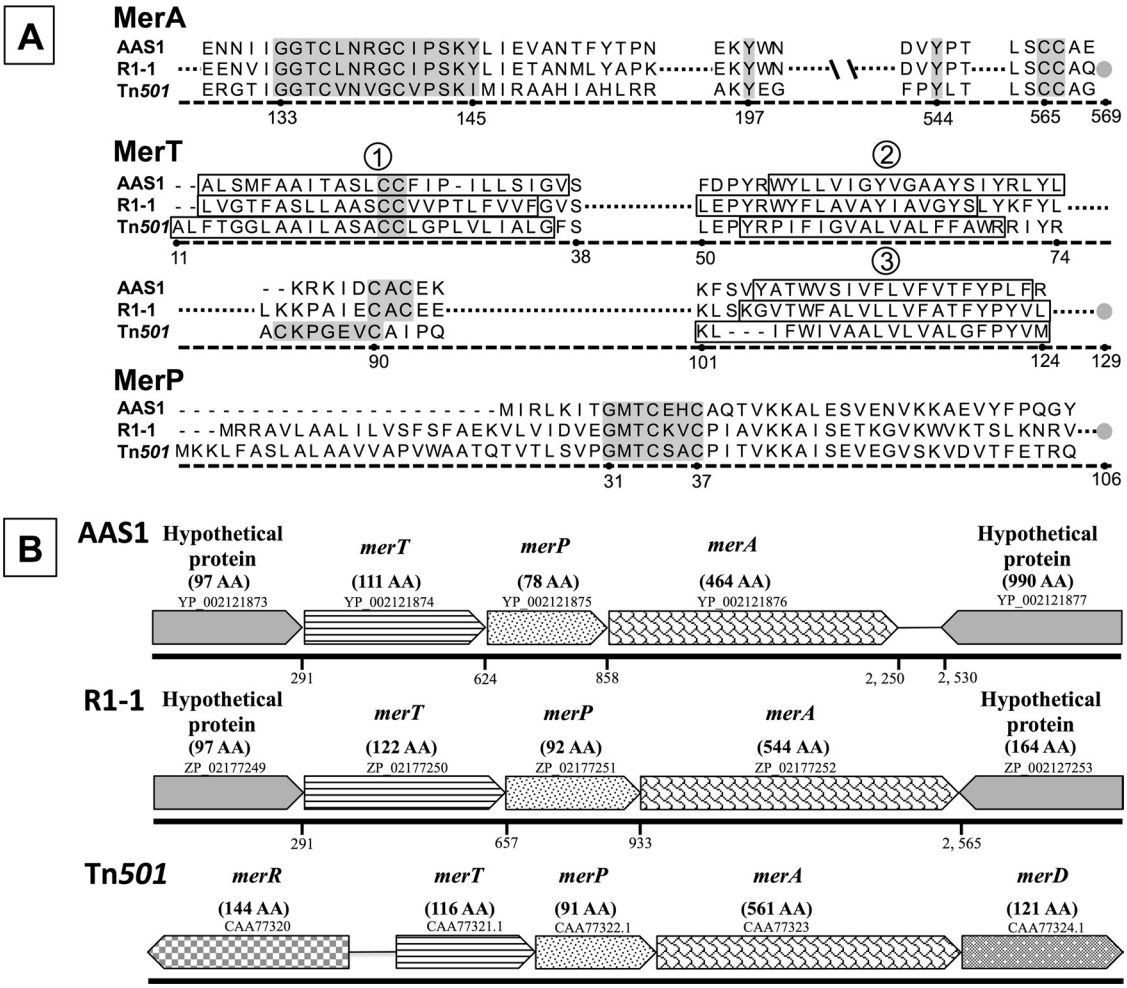

FIG 1 (A) Alignment of putative Mer proteins, including MerA, MerT, and MerP from *Hydrogenobaculum* sp. Y04AAS1 (AAS1) and *Hydrogenivirga* sp. 128-5-R1-1 (R1-1), with *mer* sequences from *Pseudomonas aeruginosa* Tn*501* as a reference. Highlighted conserved regions of functional importance (3) are as follows: for MerA, the redox active site, two downstream tyrosines, and the carboxy terminus-vicinal CC pair; for MerT, the conserved C residues in the first membrane-spanning domain and in the cytoplasmic loop between the second and third membrane-spanning domains; and for MerP, the metal binding motif GMTCxxC. The membrane-spanning domains (determined using TMpred [http://www.ch.embnet.org/software/TMPRED_form.html]) are boxed (numbered 1 to 3) in MerT. Gray circles indicate the carboxy termini of the proteins. Numbering indicates position in the Tn*501* sequence. (B) *mer* operon gene order. Arrowed boxes indicate each ORF and the direction of transcription; accession numbers are included above each box. Names of putative gene products and corresponding numbers of amino acids (AA) are given above the boxes. The numbered line below each ORF represents the nucleotide position marking the start of the gene counted from the transcription start nucleotide upstream of the hypothetical proteins in each operon.

control. Mercury forms complexes with medium components, which control its bioavailability and therefore toxicity (14). Employed growth media included either $S_2O_3^{2-}$ or H_2 as a sole energy source, leading to very different Hg(II) speciations. MINEQL+ calculations revealed that in the presence of 10 μM $HgCl_2$ and 8 mM $S_2O_3^{2-}$, Hg(II) speciated as negatively charged Hg-S_2O_3 complexes, with 84% as $Hg(S_2O_3)_2^{2-}$ and 16% as $Hg(S_2O_3)_3^{4-}$ (see Table S4 in the supplemental material). In the H_2 growth media, Hg speciated as uncharged $HgCl_2$ and HgCl(OH) complexes. The model suggested similar Hg speciation in the range of 2 to 60 μM added $HgCl_2$ (data not shown).

Using H_2 and $S_2O_3^{2-}$ as electron donors, the lowest tested $HgCl_2$ concentrations, 2 μM and 5 μM, respectively, completely inhibited growth of the control *P. marina* EX-H1, while *Hydrogenobaculum* sp. Y04AAS1 grew in the presence of 10 and 20 μM $HgCl_2$ in the H_2 and $S_2O_3^{2-}$ media, respectively, and *Hydrogenivirga* sp. 128-R1-1 grew in 20 μM $HgCl_2$ in $S_2O_3^{2-}$ medium (see Fig. S2 in the supplemental material). While it is clear that the two strains with putative *mer* operons had a higher tolerance to Hg than the control strain, it was impossible to quantitatively compare their responses or to assess the effects of electron donor and Hg speciation on the level of Hg resistance due to variable Hg loss from uninoculated $S_2O_3^{2-}$-amended media (see Fig. S3 in the supplemental material; see also below).

Loss of Hg(II) during growth of strains AAS1 and R1-1. To determine if growth of strains AAS1 and R1-1 was related to the removal of Hg(II) from growth media, changes in Hg(II) concentrations were monitored during growth to stationary phase (Fig. 2). Growth experiments were performed using 5 or 10 μM $HgCl_2$ in media containing H_2 or $S_2O_3^{2-}$, respectively—concentrations that inhibited, though did not abolish, growth in either medium (see Fig. S2 in the supplemental material).

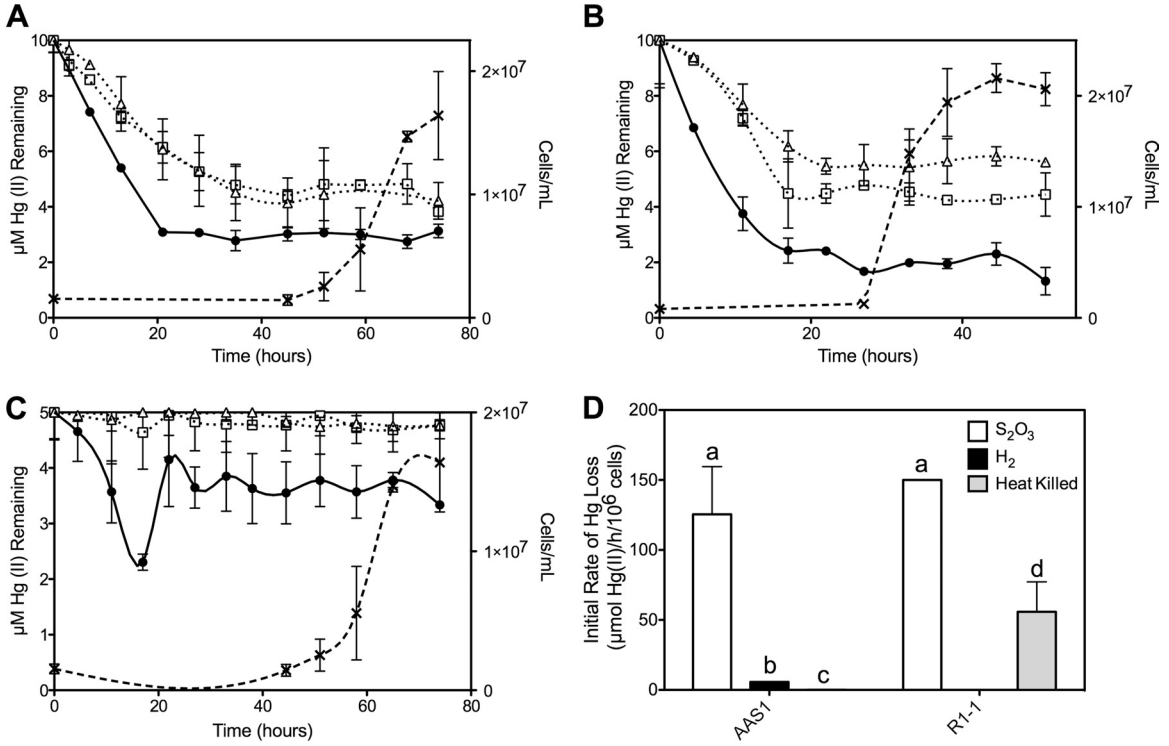

FIG 2 ^{203}Hg(II) remaining in media during growth of strains AAS1 (A and C) and R1-1 (B) using $S_2O_3^{2-}$ (A and B) and H_2 (C) as electron donors. Cell density (×) is shown, as is loss of Hg(II) (in μM) from growing cultures (●), heat-killed controls (□), and uninoculated controls (△). (D) Initial rates of Hg(II) loss [μmol Hg(II)/h/10^6 cells] calculated for strains AAS1 and R1-1 in cultures grown on $S_2O_3^{2-}$ or H_2 and for heat-killed controls. Different letters indicate statistical significance ($P < 0.05$). All data represent the mean Hg(II) loss of triplicate growing cultures ± 1 standard deviation (SD) after subtracting loss rates of uninoculated controls.

Loss of ^{203}Hg(II) from all growth media occurred well before the commencement of growth by strains R1-1 and AAS1. Initial rates of Hg loss from inoculated media were calculated after subtracting loss from uninoculated controls (see below). For strain AAS1, loss was approximately 25-fold faster when strains were grown on $S_2O_3^{2-}$ rather than H_2, with initial rates of Hg(II) loss of 125.5 ± 34.1 and 5.7 ± 0.03 μmol Hg(II) lost h^{-1} 10^6 $cells^{-1}$, respectively ($P < 0.02$ [Fig. 2D]). This is not surprising considering the higher energy yield from the oxidation of $S_2O_3^{2-}$ ($\Delta G° = -818.3$ kJ/reaction) than from that of H_2 ($\Delta G° = -237$ kJ/reaction) and the dependency of Hg(II) reduction by MR on availability of reducing equivalents (4). Strain R1-1 lost Hg(II) at a rate of 150.0 ± 0.01 μmol Hg(II) h^{-1} 10^6 $cells^{-1}$, statistically indistinguishable from the rate of strain AAS1 grown on $S_2O_3^{2-}$. Interestingly, more Hg was lost from the heat-killed controls of strain R1-1 than from the uninoculated controls ($P < 0.02$) at a rate that was slightly, though significantly ($P = 0.05$), higher. Since autoclaving (105°C for 30 min) resulted in cell death, as indicated by failure to grow following such treatment (data not shown), the MR of strain R1-1 must be highly tolerant to heat.

In the $S_2O_3^{2-}$-amended media, significant amounts of ^{203}Hg(II) were lost ($P < 0.05$) from the heat-killed and uninoculated controls (see Fig. S3 in the supplemental material) that were incubated at 55°C (strain AAS1 controls [Fig. 2A]) and 70°C (strain R1-1 controls [Fig. 2B]). At the commencement of growth, medium-only controls of strain AAS1 (at >40 h postinoculation) and R1-1 (at >20 h) had only 4.8 ± 1.3 and 5.4 ± 1.4 μM Hg(II) remaining in the media, respectively, approximately half of the starting concentration. No such loss was observed in the H_2-supplemented medium. Since loss did not occur when $S_2O_3^{2-}$ medium-only controls were incubated at room temperature (data not shown), this abiotic loss resulted from elevated temperatures. This suggests that uncharged Hg(II) complexes are less volatile at elevated temperatures than the charged Hg-S_2O_3 complexes. Nevertheless, the live growing cultures of both strains lost a significantly greater proportion of ^{203}Hg(II) than all abiotic controls ($P < 0.05$).

The Hg concentration in H_2-amended AAS1 cultures initially declined, then increased at 20 h following inoculation, and then remained stable at about 3 μM (Fig. 2C). Since incubations were carried out in closed systems where the formed gaseous Hg(0) likely partitioned between the medium and the headspace according to Henry's coefficient (at 35°C, $k_H' = 0.4$ dimensionless [1]), it is possible that some of the initially formed Hg(0) was oxidized to Hg(II) by the H_2-metabolizing culture. Bacterial Hg(0) oxidation has been reported for *Escherichia coli*, *Bacillus subtilis*, and *Streptomyces venezuelae* and attributed to the enzymes catalase and hydroperoxidase (45). The results clearly show that cultures of *Hydrogenivirga* sp. 128-R1-1 and *Hydrogenobaculum* sp. Y04AAS1 removed Hg from their growth media and that most of this activity took place during the lag phase of growth.

Production of Hg(0) by growing cultures of AAS1 and R1-1. Endpoint mass balance experiments determined that the Hg(II) which was lost during growth of strains AAS1 and R1-1 was converted to Hg(0) (Table 1). When grown to early stationary phase on $S_2O_3^{2-}$, strains AAS1 and R1-1 produced 3.8 ± 2.4 and 3.1 ±

TABLE 1 Reduction of Hg(II) to Hg(0) by *Aquificae* cultures[a]

Strain	Electron donor	Treatment	Medium Hg (μM)[b]	Headspace Hg (μM)
AAS1	H_2	Growing cultures	3.91 ± 0.18[A]	2.19 ± 0.79[D]
		Heat killed	4.32 ± 0.80[A]	0.21 ± 0.06[E]
	$S_2O_3^{2-}$	Growing cultures	5.02 ± 1.47[A]	3.80 ± 2.38[D]
		Heat killed	10.87 ± 2.60[B]	0.34 ± 0.03[F]
R1-1	$S_2O_3^{2-}$	Growing cultures	6.69 ± 0.48[C]	3.09 ± 1.34[D]
		Heat killed	8.13 ± 0.48[B]	0.32 ± 0.01[F]

[a] Different letters indicate statistical significance ($P < 0.05$) by Student's *t* test.
[b] $HgCl_2$ was added to initial concentrations of 5 and 10 μM to H_2- and $S_2O_3^{2-}$-containing growth media, respectively.

1.3 μmol Hg(0), respectively. When grown on H_2, strain AAS1 produced 2.2 ± 0.8 μmol Hg(0), statistically similar to the amount produced by $S_2O_3^{2-}$-grown cultures. Production of Hg(0) by heat-killed controls was approximately 10-fold lower than that by growing cultures for all treatments. Mass balance calculations showed recoveries of 85 to 122% of the added $^{203}HgCl_2$.

MR activities by crude cell extracts of strains AAS1 and R1-1. Specific rates of MR activity were measured to determine this enzyme's role in the formation of Hg(0) by *Hydrogenobaculum* sp. Y04AAS1 and *Hydrogenivirga* sp. 128-R1-1. Preliminary experiments indicated a preference for NADH by R1-1 and for NADPH by AAS1 crude cell extracts (data not shown), and therefore all further experiments were performed with each strain's preferred reductant. Given the developing understanding of the importance of *mer* in thermophilic microbes (2, 40, 51), MR activities of strains AAS1 and R1-1 were determined at a range of temperatures. Results showed a correspondence between optimal temperatures for growth and for Hg-dependent NAD(P)H oxidation with maximum apparent specific MR activity for AAS1 (37.7 ± 1.1 mU mg protein^{-1}) at 50°C and for R1-1 (3.2 ± 0.2 mU mg protein^{-1}) at 70°C (Fig. 3). Strain AAS1's MR was active at a temperature range of 30 to 70°C and that of strain R1-1 was active from 60 to 87°C, and both extracts had very low activities below 40°C. MR activity was not detected in crude extracts of the control

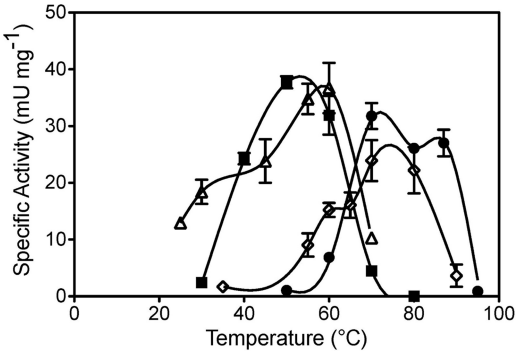

FIG 3 Effect of temperature on MR activities. Specific activities of crude cell extracts were determined for *Hydrogenobaculum* sp. Y04AAS1 (■) and *Hydrogenivirga* sp. 128-5-R1-1 (●). Activities of R1-1 extracts are expressed as those measured, multiplied by 10. Previously reported data for *T. thermophilus* (◇) and Tn*501* (△) (51) are included for comparison. Averages of three to five replicate assays ± 1 SD are presented. One unit of MR activity = 1 μmol NAD(P)H oxidized min^{-1}.

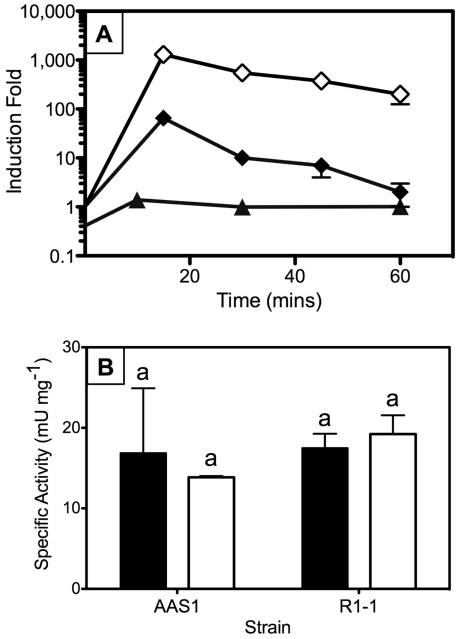

FIG 4 *merA* expression in *Hydrogenobaculum* sp. Y04AAS1 and *Hydrogenivirga* sp. 128-5-R1-1. (A) $HgCl_2$-dependent (1 μM) transcription fold induction in strain AAS1 (▲) grown on H_2 compared with induction of *merA* of HB27 (◆) and Tn*501* (◇). Fold induction was calculated as described in Materials and Methods, except that *merA* expression in Tn*501* and HB27 was normalized to expression of 16S rRNA genes rather than to *gyrA* (data from reference 51). (B) Effect of growth in the presence of Hg on MR specific activities in crude cell extracts of strains AAS1 and R1-1. Cell extract activities were determined for cultures grown with (filled column) or without (clear column) 10 μM $HgCl_2$ in $S_2O_3^{2-}$-amended media. The means ± 1 SD of triplicate determinations are shown. The same letters above columns indicate no significant difference by Student's *t* test ($P > 0.05$).

strain *P. marina* EX-H1 when tested at its optimal growth temperature, 70°C. These results suggest that strains AAS1 and R1-1 possessed thermophilic MR.

Induction of *merA* transcription and MR activity. *mer* operon expression is regulated in both *Bacteria* (47) and *Archaea* (39) by the regulatory protein MerR and, less frequently, by ArsR/SmtB-like regulators; most *mer* operons code for these regulators (3). Because gene homologs of these regulators were not found in proximity to *merA* of strains AAS1 and R1-1, we determined the effects of growth in the presence of $HgCl_2$ on levels of *merA* transcription and on MR specific activities. Results for H_2-grown *Hydrogenobaculum* sp. Y04AAS1 clearly showed that exposure to subtoxic concentrations of Hg (1 μM) did not induce *merA* expression, as indicated by a relative fold induction of 1 for the first 60 min following exposure (Fig. 4A). In contrast, *merA* expression in *T. thermophilus* HB27 and in *E. coli* carrying a chromosomal insertion of Tn*501* was induced 65- and 1,300-fold, respectively, relative to expression of the 16S rRNA gene (51). Unfortunately, transcript quantitation was not possible for thiosulfate-grown cultures due to the low quality of cDNA preparations. In such cultures, however, similar levels of MR activity were observed in crude cell extracts of cultures that had been grown with or without $HgCl_2$, with values of 17.5 ± 1.8 and 19.2 ± 1.3 mU mg protein^{-1} and 16.9 ± 8.0 and 13.6 ± 0.2 mU mg protein^{-1} for Hg-exposed and unexposed R1-1 and AAS1 cultures, respectively (Fig. 4B).

We conclude that unlike the majority of previously described

mer systems (3), expression of *mer* in strains AAS1 and R1-1 was not induced by exposure to Hg(II). The *mer* operon of the plasmid pMERPH does not include an adjacent *merR*, though its expression is inducible, likely associated with a regulatory gene located elsewhere on the plasmid (29a). A constitutively expressed Hg-dependent NADH oxidation was recently described for the marine methylotroph *Methylococcus capsulatus* (Bath) (5a). Mercury-independent expression of *mer* among the *Aquificae* may not be surprising considering that members of this phylum often occupy sulfide-rich geothermal environments (19) where Hg levels were reported at nanomolar to micromolar concentrations (21, 50). Obviously, an elaborate regulatory system would be superfluous in environments with persistent exposure to Hg.

Evolutionary implications. Phylogenetic reconstructions consistently place *Aquificae* sequences in a basal position to all bacterial and archaeal MerA proteins (see Fig. S1 in the supplemental material) (2). Thus, our results suggest that the expression of the ancestral Hg detoxification system, which likely originated among thermophilic bacteria in geothermal environments, is not regulated by exposure to Hg. If so, Hg-dependent regulation of this system was likely acquired later, possibly among organisms only intermittently exposed to toxic levels of Hg. We have previously pointed out the increased number of *mer* functions with MerA evolution (2); the present study further clarifies this system's evolutionary path from simple operons, whose expression does not depend on exposure to Hg, to more complex and finely regulated systems (9a, 17, 45a).

Furthermore, the correspondence of optimal growth and MR activity temperatures of the two thermophilic *Aquificae* strains (Fig. 3) supports the conclusion that *merA* originated among thermophiles (2, 51). In contrast, the optimal temperature of Tn*501*'s enzyme was >20°C higher than the optimal growth temperature of *Pseudomonas aeruginosa* (Fig. 3), the mesophilic Hg-resistant bacterium from which Tn*501* was isolated (46a). It has been previously proposed that this discrepancy between the optimal growth and enzyme activity temperatures was a relic of MR evolution in high-temperature environments (51). Our results, therefore, strengthen this conclusion and the identification of high-temperature environments as the place for the origin and early evolution of the microbial Hg detoxification system (2, 48, 51).

ACKNOWLEDGMENTS

We thank Anna-Louise Reysenbach, Yitai Liu, and Gilbert Flores (Portland State University) and Eric Boyd and Seth D'Imperio (Montana State University) for help regarding culture maintenance and growth, Costatino Vetriani (Rutgers University) for providing advice, lab space, and materials, Christie Bridges (Mercer University, GA) for providing $^{203}HgCl_2$, Elisabetta Bini (Rutgers) and Anne Summers (University of Georgia) for help deciphering promoter sequences, and Bill Belden and Allison Isola (Rutgers) for advice and assistance in *merA* expression experiments. Gratitude is also extended to three anonymous reviewers whose comments helped us improve the manuscript.

The financial support of a graduate student travel award by the Thermal Biology Institute (Montana State University), small grants from the Department of Biochemisty and Microbiology, and the Graduate Program in Ecology and Evolution (Rutgers University) is acknowledged, as is grant NSF-PEET-DEB-0328326 to Anna-Louise Reysenbach.

REFERENCES

1. **Andersson ME, Gardfeldt K, Wangberg I, Stromberg D.** 2008. Determination of Henry's law constant for elemental mercury. Chemosphere **73**:587–592.
2. **Barkay T, Kritee K, Boyd E, Geesey GG.** 2010. A thermophilic bacterial origin and subsequent constraints by redox, light and salinity on the evolution of the microbial mercuric reductase. Environ. Microbiol. **12**:2904–2917.
3. **Barkay T, Miller SM, Summers AO.** 2003. Bacterial mercury resistance from atoms to ecosystems. FEMS Microbiol. Rev. **27**:355–384.
4. **Barkay T, Wagner-Döbler I.** 2005. Microbial transformations of mercury: potentials, challenges, and achievements in controlling mercury toxicity in the environment. Adv. Appl. Microbiol. **57**:1–52.
5. **Ben-David EA, Holden PJ, Stone DJ, Harch BD, Foster LJ.** 2004. The use of phospholipid fatty acid analysis to measure impact of acid rock drainage on microbial communities in sediments. Microb. Ecol. **48**:300–315.

5a. **Boden R, Murrell JC.** 2011. Response to mercury (II) ions in *Methylococcus capsulatus* (Bath). FEMS Microbiol. Lett. **324**:106–110.

6. **Boone DR, Johnson RL, Liu Y.** 1989. Diffusion of the interspecies electron carriers H_2 and formate in methanogenic ecosystems and its implications in the measurement of K_m for H_2 or formate uptake. Appl. Environ. Microbiol. **55**:1735–1741.
7. **Boyd ES, et al.** 2009. Methylmercury enters an aquatic food web through acidophilic microbial mats in Yellowstone National Park, WY. Environ. Microbiol. **11**:950–959.
8. **Brown NL, Stoyanov JV, Kidd SP, Hobman JL.** 2003. The MerR family of transcriptional regulators. FEMS Microbiol. Rev. **27**:145–163.
9. **Bruce KD, Osborn AM, Pearson AJ, Strike P, Ritchie DA.** 1995. Genetic diversity within mer genes directly amplified from communities of non-cultivated soil and sediment bacteria. Mol. Ecol. **4**:605–612.

9a. **Champier L, Duarte V, Michaud-Soret I, Coves J.** 2004. Characterization of the MerD protein from *Ralstonia metallidurans* CH34: a possible role in bacterial mercury resistance by switching off the induction of the *mer* operon. Mol. Microbiol. **52**:1475–1485.

10. **Chatziefthimiou AD, Crespo-Medina M, Wang Y, Vetriani C, Barkay T.** 2007. The isolation and initial characterization of mercury resistant chemolithotrophic thermophilic bacteria from mercury rich geothermal springs. Extremophiles **11**:469–479.
11. **Craw D.** 2005. Potential anthropogenic mobilisation of mercury and arsenic from soils on mineralised rocks, Northland, New Zealand. J. Environ. Manage. **74**:283–292.
12. **Crespo-Medina M, et al.** 2009. Adaptation of chemosynthetic microorganisms to elevated mercury concentrations in deep-sea hydrothermal vents. Limnol. Oceanogr. **54**:41–49.
13. **Cuebas M, Sannino D, Bini E.** 2011. Isolation and characterization of arsenic resistant *Geobacillus kaustophilus* strain from geothermal soils. J. Basic Microbiol. **51**:364–371.
14. **Farrell RE, Germida JJ, Huang PM.** 1990. Biotoxicity of mercury as influenced by mercury(II) speciation. Appl. Environ. Microbiol. **56**:3006–3016.
15. **Ferguson TJ, Mah RA.** 1983. Isolation and characterization of an H_2 oxidizing thermophilic methanogen. Appl. Environ. Microbiol. **45**:265–274.
16. **Fox B, Walsh CT.** 1982. Mercuric reductase: purification and characterization of a transposon-encoded flavoprotein containing an oxidation-reduction-active disulfide. J. Biol. Chem. **257**:2498–2503.
17. **Guo HB, et al.** 2010. Structure and conformational dynamics of the metalloregulator MerR upon binding of Hg(II). J. Mol. Biol. **398**:555–568.
18. **Hofmann K, Stoffel W.** 1993. TMbase—a database of membrane spanning proteins segments. Biol. Chem. Hoppe-Seyler **374**:166.
19. **Huber R, Eder W.** 2006. *Aquificales*, p 925–938. *In* Dworkin M, Falkow S (ed), The prokaryotes, vol 7. Springer Reference, New York, NY.
20. **Jackson WJ, Summers AO.** 1982. Biochemical characterization of $HgCl_2$-inducible polypeptides encoded by the *mer* operon of plasmid R100. J. Bacteriol. **151**:962–970.
21. **King SA, et al.** 2006. Mercury in water and biomass of microbial communities in hot springs of Yellowstone National Park, USA. Appl. Geochem. **21**:1868–1879.
22. **Ledwidge R, et al.** 2005. NmerA, the metal binding domain of mercuric ion reductase, removes Hg(II) from proteins, delivers it to the catalytic core, and protects cells under glutathione-depleted conditions. Biochemistry **44**:11402–11416.
23. **Madigan MT, Martinko JM, Stahl DA, Clark DP.** 2010. Brock biology of microorganisms, 13th ed. Pearson/Benjamin Cummings, San Francisco, CA.
24. **Martell AE, Smith RM.** 1974. Critical stability constants. Plenum Press, New York, NY.

25. Reference deleted.
26. **Ní Chadhain SM, Schaefer J, Crane S, Zylstra GJ, Barkay T.** 2006. Analysis of mercuric reductase (*merA*) gene diversity in an anaerobic mercury-contaminated sediment enrichment. Environ. Microbiol. **8**:1746–1752.
27. **Nies DH.** 2003. Efflux-mediated heavy metal resistance in prokaryotes. FEMS Microbiol. Rev. **27**:313–339.
28. **Nies DH.** 1999. Microbial heavy-metal resistance. Appl. Microbiol. Biotechnol. **51**:730–750.
29. **Øregaard G, Sørensen SJ.** 2007. High diversity of bacterial mercuric reductase genes from surface and sub-surface floodplain soil (Oak Ridge, USA). ISME J. **1**:453–467.

29a. **Osborn AM, Bruce KD, Ritchie DA, Strike P.** 1996. The mercury resistance operon of the IncJ plasmid pMERPH exhibits structural and regulatory divergence from other Gram-negative *mer* operons. Microbiology **142**:337–345.

30. **Pfaffl MW.** 2001. A new mathematical model for relative quantification in real-time RT-PCR. Nucleic Acids Res. **29**:e45. doi:10.1093/nar/29.9.e45.
31. **Phelps D, Buseck PR.** 1980. Distribution of soil mercury and the development of soil mercury anomalies in the Yellowstone geothermal area, Wyoming. Econ. Geol. **75**:730–741.
32. Reference deleted.
33. **Reese MG.** 2001. Application of a time-delay neural network to promoter annotation in the *Drosophila melanogaster* genome. Comput. Chem. **26**:51–56.
34. **Reysenbach A-L, et al.** 2009. Complete and draft genome sequences of six members of the *Aquificales*. J. Bacteriol. **191**:1992–1993.
35. **Rosen BP.** 2002. Transport and detoxification systems for transition metals, heavy metals and metalloids in eukaryotic and prokaryotic microbes. Comp. Biochem. Physiol. A Mol. Integr. Physiol. **133**:689–693.
36. **Rossy E, et al.** 2004. Is the cytoplasmic loop of MerT, the mercuric ion transport protein, involved in mercury transfer to the mercuric reductase? FEBS Lett. **575**:86–90.
37. **Schaefer J, Letowski J, Barkay T.** 2002. *mer*-mediated resistance and volatilization of Hg(II) under anaerobic conditions. Geomicrobiol. J. **19**:87–102.
38. **Schecher WD, McAvoy D.** 1994. MINEQL+: a chemical equilibrium program for personal computers. Environmental Research Software, Howell, ME.
39. **Schelert J, et al.** 2004. Occurrence and characterization of mercury resistance in the hyperthermophilic archaeon *Sulfolobus sulfataricus* by use of gene disruption. J. Bacteriol. **186**:427–437.
40. **Schelert J, Drozda M, Dixit V, Dillman A, Blum P.** 2006. Regulation of mercury resistance in the crenarchaeote *Sulfolobus solfataricus*. J. Bacteriol. **188**:7141–7150.
41. **Shima S, Suzuki KI.** 1993. *Hydrogenobacter acidophilus* sp. nov., a thermoacidophilic, aerobic, hydrogen-oxidizing bacterium requiring elemental sulfur for growth. Int. J. Syst. Evol. Microbiol. **43**:703–708.
42. **Silver S, Phung LT.** 2005. A bacterial view of the periodic table: genes and proteins for toxic inorganic ions. J. Ind. Microbiol. Biotechnol. **32**:587–605.
43. **Simbahan J, et al.** 2005. Community analysis of a mercury hot spring supports occurrence of domain-specific forms of mercuric reductase. Appl. Environ. Microbiol. **71**:8836–8845.
44. Reference deleted.
45. **Smith T, Pitts K, McGarvey JA, Summers AO.** 1998. Bacterial oxidation of mercury metal vapor, Hg(0). Appl. Environ. Microbiol. **64**:1328–1332.

45a. **Song LY, Teng Q, Phillips RS, Brewer JM, Summers AO.** 2007. 19F-NMR reveals metal and operator-induced allostery in MerR. J. Mol. Biol. **371**:79–92.

46. **Spear JR, Walker JJ, McCollom TM, Pace NR.** 2005. Hydrogen and bioenergetics in the Yellowstone geothermal system. Proc. Natl. Acad. Sci. U. S. A. **102**:2555–2560.

46a. **Stanisich VA, Bennett PM, Richmond MH.** 1977. Characterization of a translocation unit encoding resistance to mercuric ions that occurs on a nonconjugative plasmid in *Pseudomonas aeruginosa*. J. Bacteriol. **129**:1227–1233.

47. **Summers AO.** 1986. Organization, expression, and evolution of genes for mercury resistance. Annu. Rev. Microbiol. **40**:604–634.
48. **Vetriani C, et al.** 2005. Mercury adaptation among bacteria from a deep-sea hydrothermal vent. Appl. Environ. Microbiol. **71**:220–226.
49. **Vetriani C, Speck MD, Ellor SV, Lutz RA, Starovoytov V.** 2004. *Thermovibrio ammonificans* sp. nov., a thermophilic, chemolithotrophic, nitrate-ammonifying bacterium from deep-sea hydrothermal vents. Int. J. Syst. Evol. Microbiol. **54**:175–181.
50. **Wang Y, et al.** 2011. Environmental conditions constrain the distribution and diversity of archaeal *merA* in Yellowstone National Park, Wyoming, USA. Microb. Ecol. **62**:739–752.
51. **Wang Y, Freedman Z, Lu-Irving P, Kaletsky R, Barkay T.** 2009. An initial characterization of the mercury resistance (*mer*) system of the thermophilic bacterium *Thermus thermophilus* HB27. FEMS Microbiol. Ecol. **67**:118–129.